

NASA CONTRACT NASW-96019

A VERSATILE PLANETARY RADIO SCIENCE MICRORECEIVER

FINAL REPORT

**FOR THE PERIOD
OCTOBER 8, 1996 TO OCTOBER 7, 1999**

P.I.: DR. C. D. FRY

Exploration Physics International, Inc.

Signed: Craig D. Fry, Oct 26, 1999

CO-I.: PROF. T. J. ROSENBERG

University of Maryland at College Park

Prepared October 26, 1999.

**A VERSATILE PLANETARY RADIO SCIENCE MICRORECEIVER
FINAL REPORT**

TABLE OF CONTENTS

1.0 PROJECT ACCOMPLISHMENTS	1
1.1 Project Overview	1
1.2 Background	1
1.3 Accomplishments	4
2.0 ACTIVITIES BY YEAR	4
2.1 Year 1 Activities	4
2.2 Year 2 Activities	9
2.4 Year 3 Activities	11
5.0 SUMMARY	15
REFERENCES	16
ATTACHMENT	19

Paper: A Programmable Riometer for Earth or Mars

1.0 PROJECT ACCOMPLISHMENTS

1.1 Project Overview.

This report describes work accomplished under NASA Contract NASW-96019, "A Versatile Planetary Radio Science Micro-Receiver," awarded by NASA's Planetary Instruments Definition and Development Program. The purpose of this 3-year effort was to define, design, develop and demonstrate a multi-function, high-frequency (HF) radio receiver system for planetary science investigations, and specifically for Mars surface operations. Exploration Physics International, Inc. (EXPI), teamed with the University of Maryland, College Park (UMCP) on this project. Data Design Corp. also provided hardware and software consulting services during Years 2 and 3. As originally planned, the microreceiver would incorporate the functionality of two instruments: 1) a fixed-frequency Relative Ionospheric Opacity Meter (riometer); and 2) a variable-frequency broadband receiver (BBR). The scope of the project was modified to include definition of improvements to the microreceiver that would enable it to operate in an additional third mode - as the receiver portion of an ionospheric radar (ionosonde). These instrument modes are described in the next section.

Our approach was to first design the microreceiver for terrestrial operation, and then develop and demonstrate it in field conditions. We sought to achieve a greater than ten-fold reduction in size, mass and power consumption over currently operating terrestrial systems. At the same time, we set about defining the likely RF propagation environment the sensor must operate in when deployed *on the surface of Mars*. The environmental definition was used to develop an instrument design suitable for a Discovery-class, Mars Surveyor or New Millennium Mars mission.

We had originally planned to implement the receiver design on a multi-chip module (MCM) after building a breadboard-level instrument using traditional discrete components. In this way we hoped to achieve significant reductions in size and mass over currently operating riometer and BBR instruments. However, in the design phase, we found we could utilize an Altera field-programmable gate array (FPGA) device to immediately implement some of the functionality of the breadboard components onto a single integrated circuit. By eliminating the multi-chip module implementation and testing tasks in Years 2 and 3, we could instead apply labor hours to ionosonde receiver definition and design. Many of the necessary modifications would be made to the programmed logic (i.e., software) in the detector gate array.

The various instrument modes are described in this section following some background information. We discuss project accomplishments in Section 1.3, and describe each year's activities in more detail in Section 2. The receiver theory of operation, design, operating specifications and test results are thoroughly described in Fry *et al.* (1999a), which has been accepted for publication by *Radio Science*, and attached as part of this Final Report.

1.2 Background

The Planetary Surface Instruments Workshop (Meyer *et al.*, 1995) identified radio sounding as a practical technique for observing the Martian ionosphere and middle atmosphere. The

Martian ionosphere is fairly substantial during the day, with electron densities peaking around 1 to $2 \times 10^5 \text{ cm}^{-3}$ at an altitude of $\sim 135 \text{ km}$, giving ionospheric critical frequencies of ~ 3 to 4 MHz. Maximum electron densities drop to $\sim 10^3 \text{ cm}^{-3}$ at night. Long-wave (frequencies below 30 MHz) radio science instruments have flown on many interplanetary missions and have provided new understanding of interplanetary and planetary plasma processes (Kaiser, 1977; Bougeret *et al.*, 1995). However, concepts for *surface-based* sensing of the Martian ionosphere by means of high-frequency (HF) radio have recently been addressed (Klimov *et al.*, 1990; Parrot *et al.*, 1996; Detrick *et al.*, 1997; Cummer and Farrell, 1999; and Melnik and Parrot, 1999). Also, Fry and Yowell, (1993; 1994), Yowell, (1996), Detrick *et al.*, (1997), Cummer and Farrell, (1999), and Melnik and Parrot, (1999) have looked at the effects of the Martian ionosphere on longwave propagation.

Riometer.

The riometer measures radio wave absorption in the ionosphere of cosmic radio noise (RF energy emitted from stars in the galaxy) as it passes through the atmosphere. It is used to study phenomena in the lower ionosphere (in the D and E regions) and also at higher altitudes in auroral latitudes (Little and Leinbach, 1959; Rosenberg and Dudeney, 1986). The riometer consists of an antenna connected to a self-calibrating receiver, and it is generally operated at a fixed frequency in the high-HF or low-VHF range, above the maximum expected ionospheric critical frequency. A signal is measured as the Earth's rotation sweeps the antenna across the radio sky. At a given local time, decreases in noise from the average or "quiet day" values indicate absorption of the signal by the ionosphere.

Our group evaluated radio frequency propagation through the Martian CO_2 atmosphere in terms of riometry (Detrick *et al.*, 1997). We looked at the effects of enhanced ionization by precipitating electrons on absorption efficiency, and found atmosphere of Mars appears even more suitable for riometry than the Earth's. We concluded that a riometer on a Mars lander (operating in the 20-30 MHz range) could be used to characterize the energy deposition due to solar energetic particles and energetic electrons impinging into the atmosphere from above.

Broadband Receiver.

Atmospheric and exo-atmospheric radio noise covers a broad spectrum (kHz to hundreds of MHz). For example, at Earth, whistlers (dispersive radio signals which travel along the Earth's magnetic field lines) are generated by lightning and can be detected on the ground by VLF receivers. Plasma processes in the terrestrial magnetosphere also generate other signals. Recently, broadband HF radio receivers have demonstrated their utility for sensing of the terrestrial ionosphere-magnetosphere and have been used to detect and study natural plasma emissions originating or passing through the bottomside ionosphere (La Belle and Weatherwax, 1992; Weatherwax *et al.*, 1994).

We know little about the natural radio emissions in the lower atmosphere of Mars. Recent studies suggest that RF emissions from Martian dust storms and dust devils might be used to measure ionospheric changes and surface conductivity (Farrell *et al.*, 1999; Cummer and Farrell, 1999). As mentioned, radio frequency receivers and electric field probes have flown on a number space missions, but none have been operated from the surface of Mars. However, this configuration is needed to characterize the in-situ radio frequency environment. This is because

signals generated in the lower atmosphere and at frequencies below the local plasma critical frequency normally cannot penetrate through the ionosphere of a weakly magnetized planet, and therefore would likely not be detected by orbiting sensors. The amplitude and spectra of the noise environment could provide new information on both the ionosphere and surface properties (Meyer *et al.*, 1995; Farrell *et al.*, 1999; Cummer and Farrell, 1999; Melnik and Parrot, 1999).

Ionosonde Receiver.

An ionospheric sounder is a radar used to measure the vertical distribution of ionospheric electrons in the ionosphere. Until recently, ionosondes required large antenna structures and significant transmitter power. However, modern electronics and signal processing techniques have considerably reduced the size, mass and power requirements of these instruments (Barry, 1971; Poole, 1985; Reinisch *et al.*, 1992).

The ionospheric regions below the electron density peak (the bottomside ionosphere) are not directly accessible by radar sounding from orbiting spacecraft (topside sounding). Several concept papers concerning Mars surface-based ionosondes have appeared (Klimov *et al.*, 1990; Fry and Yowell, 1993; Yowell, 1996; Parrot *et al.*, 1996).

Ionosondes operate in several modes. In the monostatic mode, the transmitter and receiver are collocated. A pulse is transmitted vertically and received after being refracted back to the receiver by the ionosphere. The time delay between transmitted and received signals gives the apparent, or "virtual" height of the reflecting ionospheric layer. In the bistatic mode of operation, the ionosonde transmitter and receiver are separated from each other by some distance. The upward-directed, obliquely propagated signal (at RF frequencies up to several times the critical frequency) is refracted back to the surface beyond the horizon. The measured ionospheric information is assumed to be applicable at the mid point of the ray path.

By varying the frequency of the radar pulse, a virtual height-versus-frequency chart, or "ionogram" is obtained. The electron density profile can be derived from the ionogram in a straightforward manner. Successive ionograms allow measurements of the time variations of the electron density profiles. The layer shapes and other properties of the derived profiles give an understanding of the plasma scale heights, and the constituents in each layer. Estimates of the time constants for growth and decay of ionization provide additional information about each layer and the chemistry that dominates each region. Fluctuations in heights of ionospheric layers are related to standing or traveling waves which are driven by the underlying neutral gas motion. By monitoring the distribution of fluctuation periodicity, it is possible to estimate the Brunt-Vaissala frequency of the atmosphere. This indicates the natural oscillation period of the atmosphere and leads to a measure of fundamental atmospheric properties. The radio wave attenuation as a function of frequency provides another method (in addition to the riometer) to measure radio-wave absorption in the atmosphere.

Although the ionosonde has seen long service on Earth, ionosondes have not been applied to science investigations from the surface of another planet. Cooperative operation of a topside sounder with an ionosonde receiver on a lander would effectively extend the topside sounder measurements. Topside sounders include the longwave radar on the ill-fated Mars-94 (renamed Mars-96) spacecraft (Nielsen *et al.*, 1996), and the Plasma Waves and Sounder (PWS) instrument

on the Japanese Planet-B spacecraft (Ono *et al.*, 1998) now due at Mars in 2003. A Mars topside sounder is in NASA's plans for the 2010 time frame.

1.3 Accomplishments

Results of laboratory and field tests indicate that we have met the project's primary objectives: 1) to define, design and demonstrate a miniature, multi-mode receiver for conducting radio science investigations from the surface of Mars; and 2) to reduce the mass and power over traditional instruments by a factor of ten, and without sacrificing instrument performance. The final receiver design is detailed in the attached preprint Fry *et al.* (1999a). A subsequent paper now in preparation will describe the Mars RF propagation model (Fry *et al.* (1999b).

During Year 1, we designed and built a breadboard receiver that implemented the riometer mode of operation. We implemented several of the receiver subsystems in the FPGA software. We developed a Mars HF radio propagation model for evaluating the RF environment expected on Mars. Analyses of the environmental simulations were used in the definition of the optimum receiver parameters for the Mars scenario. By the end of Year 2, we had successfully implemented both the riometer and BBR modes of operation on the same circuit board.

During Year 3, we deployed and tested the microreceiver at McMurdo Station, Antarctica. Test results were used to guide the final instrument design. Members of our team presented progress reports at a number of technical conferences and other forums.

We also defined the modifications to the microreceiver design necessary to operate the instrument as the receiver portion of a Mars surface-based ionospheric sounder. We implemented a number of these modifications. For example, we extended the broadband receiver mode's frequency range to cover the entire HF spectrum from 100 kHz to 25 MHz (low-band version), and 10 to 40 MHz (high-band version). We also modified the receiver to sweep in frequency at variable rates, including the 50 kHz/sec and 100 kHz rates necessary for tracking FMCW ionospheric sounder signals. However, we did not implement the design modifications necessary to track and process an actual sounder signal. We determined that we would need to increase the A/D sample rate and incorporate additional processing into the FPGA array. Our analysis indicated this was beyond the capabilities of the current design of the FPGA hardware/software, and would be pursued in a subsequent PIDDP opportunity.

2.0 ACTIVITIES BY YEAR

2.1 Year 1 Activities

The first year's work focused on designing and building a breadboard receiver that implemented the riometer mode of operation. We also began the RF propagation study to pin down receiver parameters for defining the Mars version of the receiver.

Receiver Design.

Efforts during the first quarter were directed toward receiver definition, focusing on two areas, environmental simulations and receiver definition/design. Modifications to the receiver design proposed by UMCP to incorporate a gate-array detector offered several benefits. The

original receiver design concept was based upon using a high-speed DSP to detect and process the baseband received signal. However, recent advances in gate array technology allow the signal processing algorithm to be implemented in hardware. This offered significant reductions in power over our original approach.

During the second quarter, work focused on the gate array detector for the riometer portion of the microreceiver. We made significant progress on the Gate Array Receiver System (GARS). Dr. Rosenberg's staff worked on developing the detector subsystem in order to evaluate its performance. They modeled the detector functions using MathCad to optimize the circuit design board and designed a signal simulator that produced quad-phase IF baseband signals. They completed the detector circuit design and built the detector board and simulator assemblies. The gate array was mated to a computer interface connector for easy design modifications.

In the third quarter, we implemented the detector DSP algorithms on an Altera gate array, finalized the riometer block diagram and developed the breadboard schematic. The clock frequency was increased to allow DSP sampling at the gate array's maximum rate. UMCP built an evaluation board to test other key receiver components, and software was developed for a PC to accept the data from the GARS through the PC serial port. Efforts continued to: 1) verify the performance of the gate array detector using the computer serial interface connector, 2) verify the detector using an existing riometer connection; and 3) complete the mechanical and electrical design of the RF front end and of the GARS. We made a direct digital connection of the detector to the computer and evaluated its performance through the serial interface. The detector was mated to an existing riometer front end and evaluated following a test plan.

During the fourth quarter, the DSP algorithm in the GARS was further developed to permit it to operate in the Altera 10K series device. Extensions were added to the design permitting uplink control of the receiver functions, such as changing the filter time constants and operating mode:

1) adjust gain, 2) noise source calibration, 3) normal acquire mode. The design of the mechanical housing for the prototype receiver was completed. We made additional breadboards containing candidate receiver design blocks and evaluated them. One example is shown in Figure 1. Receiver pc board layout was completed to fit within the constraints of the housing, and to also have a high degree of isolation between the receiver sections. The finished pc board was constructed in sections, which were tested individually.

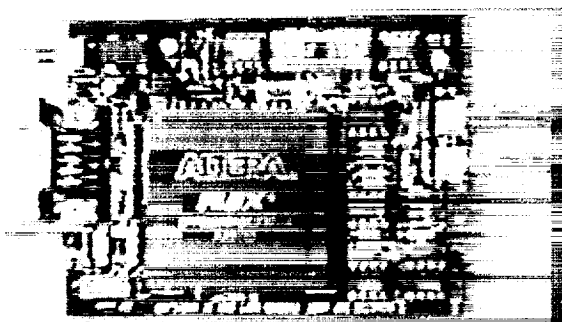


Figure 1. Detector subsystem breadboard showing the Altera gate array.

There were several advantages of the gate-array detector approach over using an embedded DSP system. There was a higher confidence that locally generated interference (due to self-emission of RF) could be minimized. Software design, development and debugging chores were reduced. Also, the pipeline design provided an opportunity for further reducing the system power consumption beyond our original proposal. We undertook the following design tasks for the receiver:

- 1) Develop signal processing algorithm
- 2) Design detector test circuit
- 3) Construct prototype detector and interface to PC
- 4) Measure detector function performance parameters
- 5) Interface gate-array detector to an existing receiver system
- 6) Design receiver by mating the RF front end to the gate-array detector

MathCad simulations permitted rapid testing of the detector algorithm in the actual gate array hardware. The MathCad results closely matched the actual data obtained from the sinusoidal and noise inputs to the gate array. The high correlation between the MathCad results and actual data was encouraging. Results suggested we had met all design requirements for the detector. Although the gate array detector consumed more power than we would like, through judicious design of the GARS, we hoped to meet the overall power goals identified in the proposal.

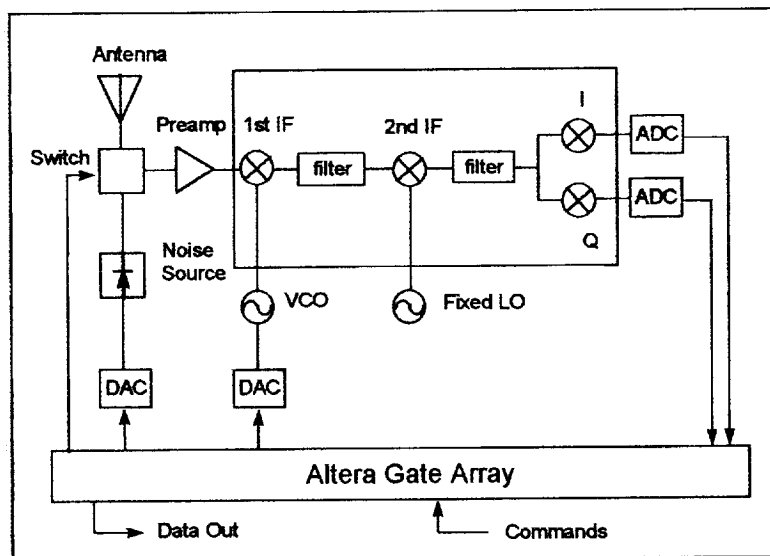


Figure 2. Block diagram of key components of the Altera Gate Array Receiver System, Year 1 design. Significant changes to the design of the GARS allowed us to use a smaller, lower power Altera gate array, without impacting detector performance. Linearity problems in the detector related to numerical truncation errors were addressed by increasing the arithmetic accuracy in the macro-functions to 32 bits.

A key aim was to evaluate the design at low values of circuit current to determine if the gain or intermodulation characteristics were degraded to unacceptable levels. We found that the preamplifier functioned well at operating currents as low as 2 ma (at 3V), and exhibited gains of up to 20 dBm with 3rd order intercept of -8 dBm. The DSP was the first section populated on the pc board. This was done to confirm that the change in design from the Altera 8K pin grid to the 10K quad flat pack unit worked as we expected. We were able to download our design file for the DSP gate array using the PC and the Altera configuration table.

Other sections of the receiver were constructed, including the preamplifier, first and second mixers, and local oscillators (LO). A problem was discovered with the second LO having insufficient drive for the second mixer. A circuit change increased the second LO drive level to solve this problem. We were able to apply an RF signal to the antenna input and trace the signal all the way to the I (in phase) and Q (quadrature) outputs of the receiver. However, there remained a problem with the first LO not properly locking to its crystal.

RF Propagation Environment Definition.

We defined the RF propagation model, to include an atmosphere/thermosphere model for neutral densities and temperatures, an ionospheric model, and an RF ray-tracing algorithm. Work began on integrating the model atmosphere and ionosphere with the ray-tracing algorithm. Figure 3 is a block diagram showing the components of the propagation model.

Neutral Atmosphere/Thermosphere Model. Mars-GRAM (Mars Global Reference Atmosphere Model) is the definitive *engineering* model for the Martian neutral atmosphere. Justus *et al.* (1996a; 1996b) described a revised Mars-GRAM with an improved thermosphere model. We contacted Mr. Dale Johnson and Ms. Bonnie James at Marshall Space Flight Center's Systems Analysis and Integration Laboratory to obtain the most current version of this model. Dr. Jere Justus provided Version 3.6 of the Mars-GRAM source code from the NASA MSFC FTP site. We implemented this new version at EXPI.

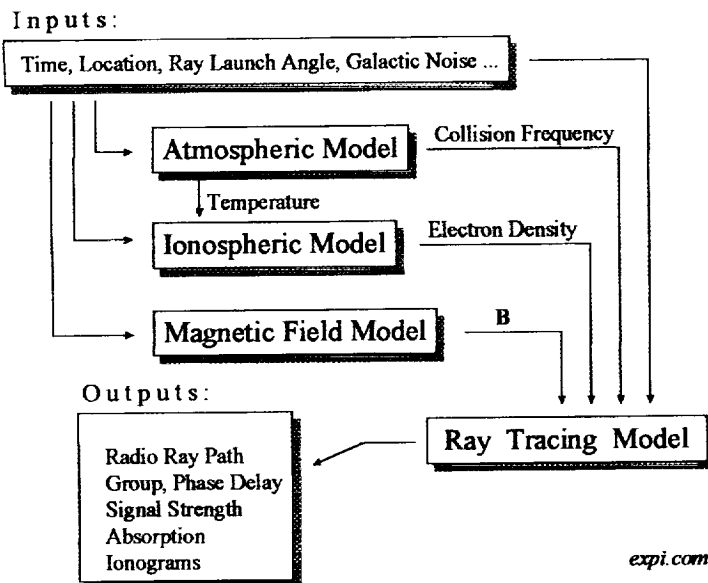


Figure 3. Block diagram of the RF Propagation Model design for the Mars environmental simulations. Inputs (top of chart) provide initial conditions for model components, and specify scenario parameters and desired outputs and output formats (bottom of chart). The (neutral) atmospheric model and ionospheric model define the propagation medium for the RF ray-tracing algorithm.

Martian Ionosphere Model. The background ionospheric model for the RF propagation analyses uses an empirical Chapman profile based upon the re-analysis of radio occultation data by Zhang, *et al.* (1990a, b). An enhanced D-region algorithm is based upon the work by Detrick *et al.* (1997). The ionospheric model provides the electron density profiles (EDPs) as a function of solar cycle ($F_{10.7}$ flux), solar zenith angle and height. The EDPs are used to determine the refractive index and its first derivative, needed in the ray-tracing algorithm. Key inputs are solar zenith angle, height, and neutral atmosphere temperature, as calculated by Mars-GRAM. The calculated electron density is used by the ray tracing algorithm to compute local refractive index, required to determine output parameters such as the path the radio ray takes through the ionosphere, group and phase delay and integrated absorption. We incorporated this ionospheric model into the ray-tracing routine as a subroutine.

HF radio propagation modeling. Since the collision frequency in CO_2 is nearly constant at temperatures characteristic on Mars, the Sen-Wyller absorption formula reduces to the Appleton-Hartree form, as discussed by Detrick *et al.* (1977). In 1997, it was thought that Mars had a

weak or non-existent intrinsic magnetic field. Therefore, we implemented a ray-tracing code (Jones and Stephenson, 1975) with the following characteristics: Appleton-Hartree formula, no magnetic field, with collisions. We obtained the source from the National Geophysical Data Center web site, as implemented by McNamara (1992). The code compiled successfully using the Microsoft Powerstation 4.0 Fortran compiler on an EXPI Pentium system. We made significant modifications to the Jones-Stephenson ray-tracing code in order to get the routines to run without error on our computer system. These changes included standardizing the initialization statements and I/O calls between the various subroutines. Work proceeded on implementing and coupling the neutral atmosphere and ionospheric models into the Mars RF propagation model. We became familiar with the neutral atmosphere model (Mars-GRAM) and the ray-tracing algorithms.

Although Mars-GRAM compiled and ran without a hitch, getting the Jones-Stephenson ray-tracing algorithm to run consistently presented us with a considerable challenge. We evaluated our implementation of the ray-tracing code by comparing modeled ray paths with exact results provided by a reference quasi-parabolic electron density profile (Croft and Hoogasian, 1968).

The code performed as expected for ray paths near the horizon, but we experienced problems for runs at higher take-off angles, which we suspected were related to the handling by the compiler we were using (Microsoft Powerstation 32-Bit Fortran) of complex variables. We were able to debug the code, and have confirmed it performs satisfactorily at all takeoff angles. This took longer than anticipated. However, it was important that it be done properly so that it can be used to accurately pin down the final (Mars version) receiver design parameters.

Year 1 Meetings.

We held an initial project meeting on December 4, 1996, at the University of Maryland at College Park (UMCP), with the key participants attending. The group reviewed the schedule, deliverables, and task list. Mr. John Giganti (UMCP Physics Department Electronic Development Group) presented recommendations for improving the receiver design using gate-array logic devices in lieu of the Digital Signal Processor (DSP) detector. We discussed the relative merits of this approach and decided to actively pursue this avenue early in the project. Prof. Rosenberg recommended we expand the timeline chart to clarify that the riometer development would proceed before the BBR portion of the effort.

Prof. Rosenberg, Dr. Weatherwax and Dr. Fry met in May to discuss progress on the receiver. We presented a poster paper related to this project (*HF radio propagation in the Martian ionosphere*) at the Spring American Geophysical Union meeting in Baltimore on May 29, 1997. Dr. Fry attended the Planetary Instruments Definition and Development Program Workshop in Pasadena, June 10-12, 1997 and presented a poster on our microreceiver project. He also presented a talk on this project to about 50 ham radio operators at the Fresno Amateur Radio Club meeting on June 13, 1997. We met on July 15, 1997 at UMCP to review the status of design and breadboarding the receiver, as discussed below.

2.2 Year 2 Activities

Receiver Design.

Efforts during the first quarter focused on prototyping the riometer mode of the microreceiver, and adding functionality required for the BBR and ionosonde receiver modes. We made several design changes to decrease receiver power consumption.

During the second quarter, we completed design and construction of the riometer portion of the microreceiver. Lab measurements of receiver performance characteristics indicated they met the design goals. We were satisfied that digital noise from the gate array used in the detector/DSP appeared to have no impact on receiver performance. Work continued on implementing the variable-frequency operation required by the BBR and ionosonde modes of operation, and on further decreasing the receiver power consumption.

In the third quarter, we conducted preliminary field tests of the prototype riometer mode circuit. We compared the performance of the microreceiver with the University of Maryland's present operational system, a La Jolla Scientific riometer. Work continued on implementing the broadband receiver mode into the circuit design.

During the fourth quarter, we completed the design and fabrication of the new receiver module. That version of the prototype circuit board used switched filters at the front end, and between the first and second IF stages. We replaced the dual-voltage Altera gate array part previously used, with a new 3-Volt only part. Additional changes were incorporated in the Altera gate array to enable uplink of commands over the RS232 serial input to control and configure the receiver. The uplink functions now included the ability to program the following receiver parameters: receiver frequency, IF bandwidth selection, detection time constant, and receiver mode selection (i.e., either VLF/HF receiver or riometer). The receiver module included changes needed due to dropping the lower frequency limit down to 100 kHz as required for the VLF end of the receiver operation. We tested the receiver performance over the frequency range from 100 kHz to 25 MHz.

Our lab and field tests demonstrated that the riometer mode was operating properly. Figure 4 shows results of the receiver linearity tests, indicating a linear response over a >30 dB range of input. Figure 5 shows the output of the riometer mode of operation collected at the UMCP Beltsville field site. The quiet day curve of received cosmic radio noise is clearly visible, indicating the receiver was working properly.

By incorporating the 3-V Altera part, we significantly reduced the power consumption of the receiver board. Linearity tests in the lab and preliminary field tests of the riometer mode demonstrated the receiver was performing properly. The noise figure measured a respectable 2.8 dB when operating at 25 MHz, and 5 dB at a 100 kHz operating frequency.

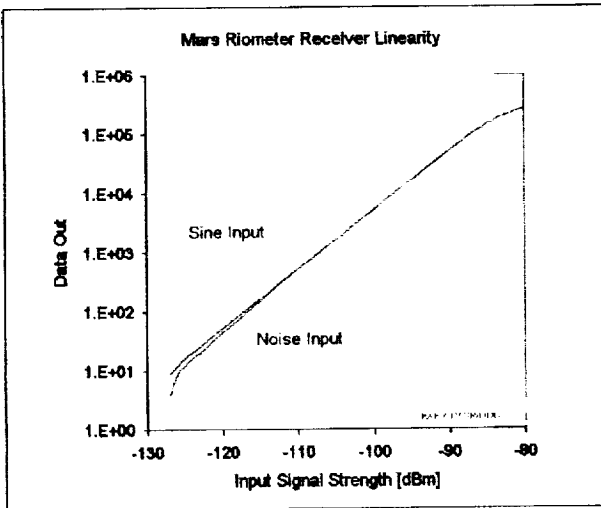


Figure 4. Laboratory measurements of detector linearity for (a) sinusoidal input and (b) a random noise source.

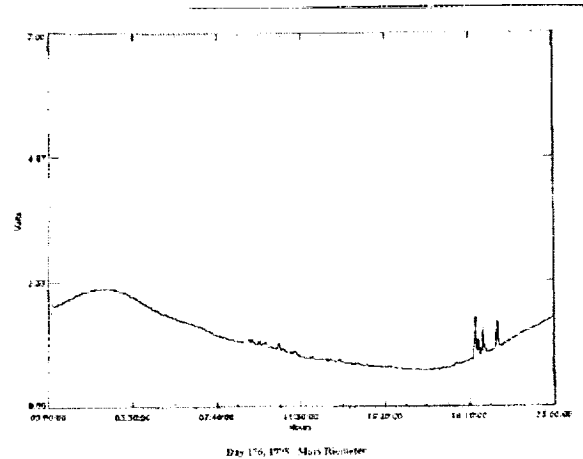


Figure 5. Sample riometer mode output showing 23 hours' data collected at the UMCP Beltsville field site.

RF propagation Environment.

We modified our HF radio propagation model to allow modeling ionosonde receiver parameters in the Martian environment. The ionospheric specification model was extended to provide a better representation of average ionospheric conditions at larger solar zenith angles (near the day/night terminator). We conducted radio propagation studies to pin down the operating parameters for the Mars version of the microreceiver. We used the Mars HF radio propagation model to evaluate the maximum usable frequency for oblique ionospheric soundings.

We looked at both vertical- and oblique-incidence ionosonde scenarios. A vertical-incidence ionosonde signal will be refracted back to the surface if the radio frequency is equal to or less than the overhead peak plasma frequency. This critical frequency is about 3 to 4 MHz during the Martian daytime. However, an obliquely propagating signal can be refracted to a distant lander at several times the critical frequency.

Our calculations indicated that an oblique ionospheric sounder should be practical even when using a relatively simple antenna. Figure 6 shows the diameter of illumination of the overhead ionosphere on Mars as a function of height, for a dipole antenna with a half-power beam width (HPBW) of 60°. At a height of about 135 km (typical height of the plasma peak density at a low-latitude location at Martian noontime), the footprint is about 450 kilometers. An appreciable fraction of the radiated RF energy will intersect the ionosphere at hundreds of kilometers distance from the zenith, and can be refracted back to the surface at double that distance beyond the horizon.

We looked at several oblique ray paths in order to determine the highest required frequency for oblique ionosonde operation. For example, Figure 7 shows the maximum usable frequency

predicted by our model over a 24-hour period (almost 1 Martian Sol) for a lander separation of 500 km.

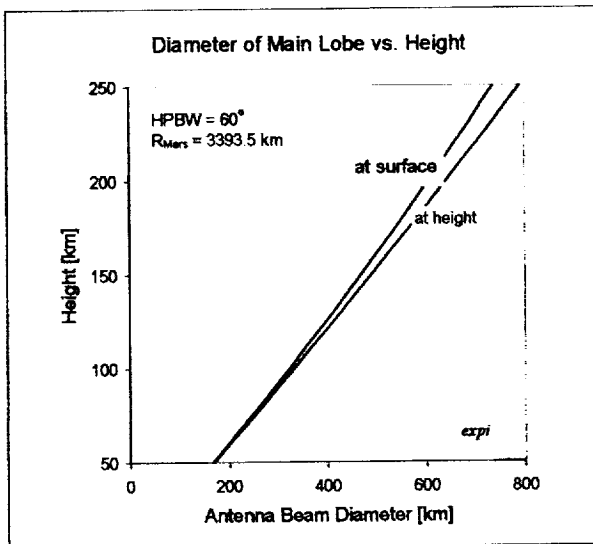


Figure 6. Diameter of antenna beam on Mars vs. height for an upward-directed antenna with a half-power beam width (HPBW) of 60°.

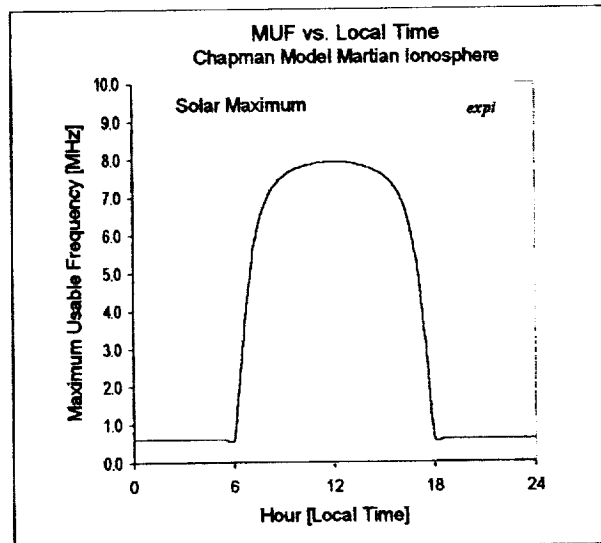


Figure 7. Maximum usable frequency for a 500 km path on Mars. The two ends of the path are near the equator, and during solar maximum conditions (in this particular case, peak electron density = $1.7 \times 10^5 \text{ cm}^{-3}$ at 135 km altitude).

Year 2 Meetings.

In January of 1998, Mr. Dan Detrick, IPST/UMCP, presented our receiver design at a meeting with Prof. Erling Nielsen's group at Max Planck Institute for Aeronomy, Lindau, Germany. As a result of discussions with Nielsen's group, we began looking at the issue of using space-qualified parts in the receiver design, or qualifying parts for which there are no substitutes. We also looked at design modifications that would be required to extend the receiver's frequency coverage to a higher frequency, up to 100 MHz. In May, Dr. Fry, Ms. Susan Fry (President of EXPI), Prof. Rosenberg and Dr. Weatherwax held a technical coordination meeting in Boston while at the Spring AGU meeting.

2.4 Year 3 Activities

During the first quarter, we completed the implementation of the broadband receiver mode of operation, and fabricated a second-generation receiver board incorporating several design modifications. We corrected some design problems uncovered during laboratory testing of the microreceiver. Programming efforts focused on the PC-based user interface to the receiver, to set modes of operation and other control functions. We tested the uplink commanding and configuration of the receiver under control of a PC over the serial interface. We developed a

Windows program using Visual Basic to serve as a graphical user interface for controlling the receiver.

Several problems cropped up during receiver testing and were corrected. The first involved a spurious output source. The source was eliminated by decoupling an unused digital output from the Maxim second mixer. The second problem involved loss of lock in the frequency synthesizer at the end of a frequency sweep. This problem was solved by modifying the gate array logic to control the rate that the synthesizer ramps back to its initial frequency. The design implementation allowed the receiver to tune smoothly over its entire frequency range without spurious emissions, and also to function properly in sweep mode.

We investigated modifications to the design to allow the receiver to acquire and track signals from a commercial FMCW ionospheric sounder. This requires matching the start time and sweep rate of the receiver with the transmitter. We increased the frequency agility of the BBR mode to allow sweeping the receiver frequency at the standard 50 kHz/sec and 100 kHz/sec rates.

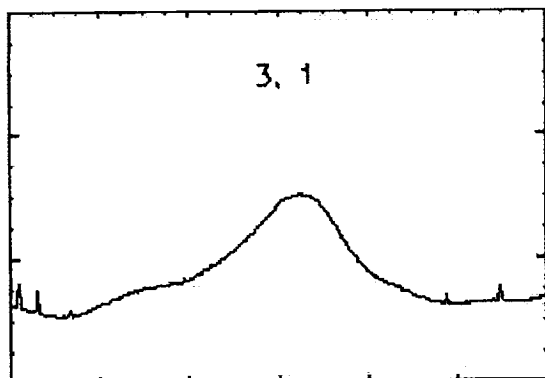
During the second quarter, we constructed two versions of the second-generation microreceiver design. The HF1-Hi version was optimized to cover the 10 to 40 MHz frequency range, while the HF1-Lo version tunes from 100 kHz to 25 MHz.

In mid-January, a microreceiver was installed at the University of Maryland's 16-beam Imaging Riometer System at McMurdo Station, Antarctica. For a discussion of imaging riometers, see for example, Detrick and Rosenberg, (1990), and Rosenberg *et al.* (1991, 1993). The microreceiver instrument was operated at 38 MHz in parallel with a traditional La Jolla Sciences, Inc., riometer and collected almost 3 weeks of data. Piggybacking on this NSF-funded trip enabled us to test the receiver in a Mars-like environment, enhancing the science return from the project.

Figures 8 and 9 show plots of relative signal strength over a 24-hour period from the McMurdo Imaging Riometer System for one of the 16 antenna beams. Observations are shown for both the La Jolla Sciences, Inc., instrument (labeled "Chivers" in Figure 8) and the microreceiver (labeled "Mars Receiver" in Figure 9). The microreceiver clearly tracked the diurnal variation in cosmic radio noise. However, an anomalous variation in signal strength was observed on the microreceiver, with periods of about 11 minutes, and longer. This variation was not observed in the broadband mode tests conducted earlier at the Beltsville, MD, facility. We believe the variation in noise level resulted from aliasing between the internal calibration cycles of the microreceiver, the beam switching and the data acquisition system. Unfortunately, the tests at McMurdo occurred during a period with few absorption events. The one small event on February 4th (observed by the La Jolla instrument and UMCP's broadband riometer) was lost in the "noise" problem affecting the microreceiver.

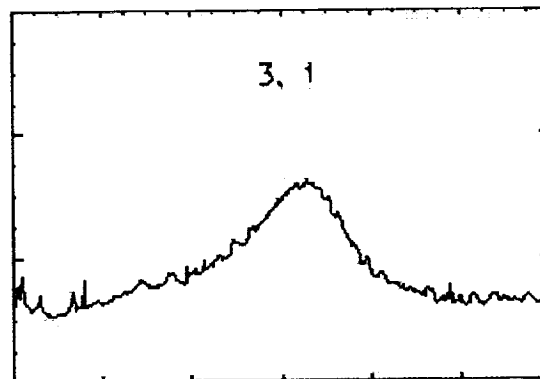
In March, we submitted a paper (attached) entitled "A Programmable Riometer for Earth and Mars" to the journal, *Radio Science*. We made several changes to the original draft to address the reviewers comments, and modified several figures to show the results in units of measurement more commonly used in the riometry community. The paper describes the microreceiver's riometer mode of operation in detail, and gives performance parameters applicable to the broadband mode, as well.

Following lab testing, an low-band prototype microreceiver was delivered to our Milford, NH office for field testing at EXPT's Amherst field site. The package included the HF1 Control Panel software (Version 2.0) for evaluation and feedback.



Chivers Riometer

Figure 8. Relative signal strength from beam 3,1 as measured by the La Jolla Sciences, Inc. riometer during the January, 1999 McMurdo field test.



Mars Riometer

Figure 9. Relative signal strength from beam 3,1 as measured by the HF1-Hi version of the microreceiver. The receiver was operating in the riometer mode and running in parallel with the La Jolla instrument.

The ionosonde receiver mode definition continued on the chirp sounder concept. Present-day commercial FMCW chirp sounders operate at ~ 10 Watts, while pulse sounders require ~ 1 kW input power, so the former type of sounder seems more practical for near-term Mars surface operation. It would be desirable to operate a Mars ionosonde as an vertical incidence ionosonde (in the monostatic radar mode). This essentially requires the transmitter and receiver to share a common antenna, and isolation between the transmitted and received signals becomes an issue. We looked at the FMCW sweep rate required to achieve acceptable isolation. We also investigated a frequency hopping scheme developed by Poole (1979) for this purpose.

During the third quarter, we opened a dialog via email with Prof. Allon Poole at Rhodes University, Grahamstown, South Africa, concerning ionosonde receiver requirements. Prof. Poole provided insights into the modulation scheme used in his advanced chirp sounder studies (Poole, 1985a, b). We also ran radio propagation simulations for Dec. 17, 2003 using our Mars RF propagation model. This scenario corresponds to NASA's projected deployment of the Mars Airplane on the 100th anniversary of the Wright Brother's Kitty Hawk flight. For example, the latitudinal variation of ionospheric critical frequency as a function of local time is shown in Figure 10. Calculations were made using our semi-empirical Chapman model of the Martian ionosphere based on model parameters presented in Zhang *et al.* (1990a), with modifications to include spherical geometry effects. A peak critical frequency of 3.8 MHz is predicted at local noon, during a hypothetical period of moderate solar activity. Figure 11 is a simulation of an ionospheric sounding ionogram for a station located at the sub-solar point (local noon with the sun directly overhead). This figure was produced using our Mars RF propagation model and a

quasi-parabolic model of the Martian ionosphere with no absorption, also during a period of moderate solar activity.

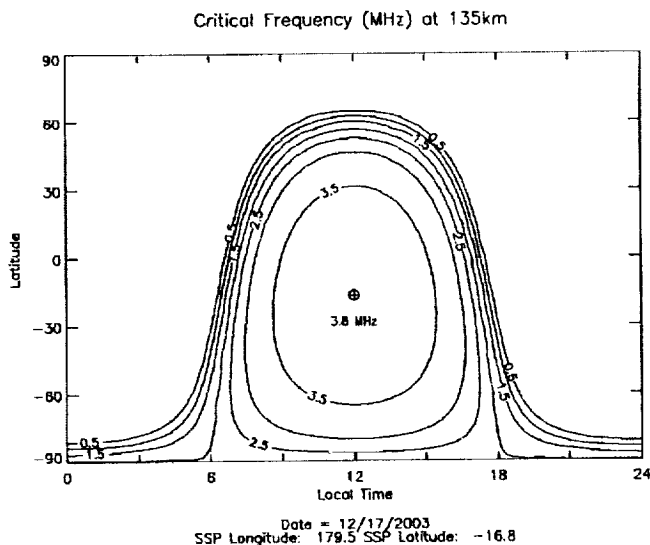
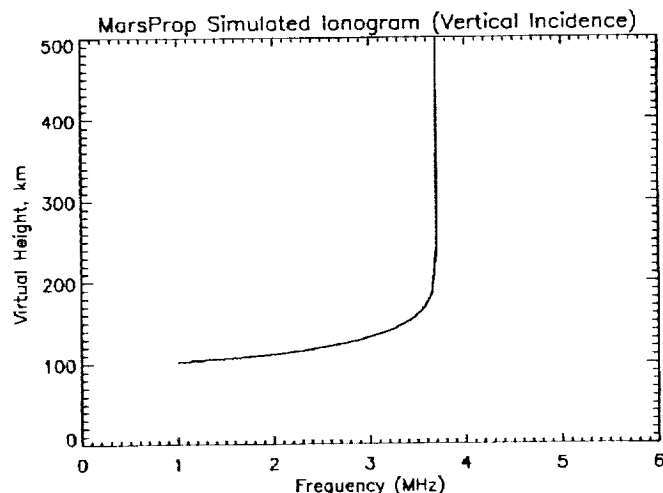


Figure 10. Plasma frequency of the Martian ionosphere at 135 km (approximately the critical frequency), as a function of local time and latitude, predicted for December 17, 2003. This corresponds to the scheduled date of deployment of the Mars Airplane.

Figure 11. Simulated ionogram (ionospheric sounding displayed as virtual height vs. frequency) for Mars. The ionogram was obtained using our RF propagation model. In this case, electron density peaks at $1.7 \times 10^5 \text{ cm}^3$ at an altitude of 135 km.



The final quarter's activities included evaluating the PC-based control software, and finalizing a set of receiver specifications for the ionosonde mode of operation. We evaluated the software interface used to control the microreceiver, and began collecting data while running the microreceiver in the broadband receiver mode. We pursued the source of the anomalous variations observed in the Mars riometer mode signal during the McMurdo test, but were not able to duplicate the problem in broadband tests. We submitted a follow-on proposal to NASA/PIDDP to extend the upper limit of the receiver's operating frequency to 100 MHz. This innovation would greatly increase the possible range of measurements of the receiver, and allow measurements of absorption during higher-energy events expected on Mars that would saturate our present receiver. We also proposed to develop an energetic particle deposition component to our ionospheric propagation model to pin down the definition of the receiver parameters for Mars

operation. The modeling is necessary in order to characterize, for the first time, cosmic radio noise absorption by the Martian ionosphere during solar proton events.

Figures 12 and 13 show the final versions of the receiver functional block diagram and circuit board. The radio receiver, calibration, data acquisition and processing, and command and control functions are all contained on a single circuit board measuring 9x14 cm. The receiver draws about 120 mw power when operating.

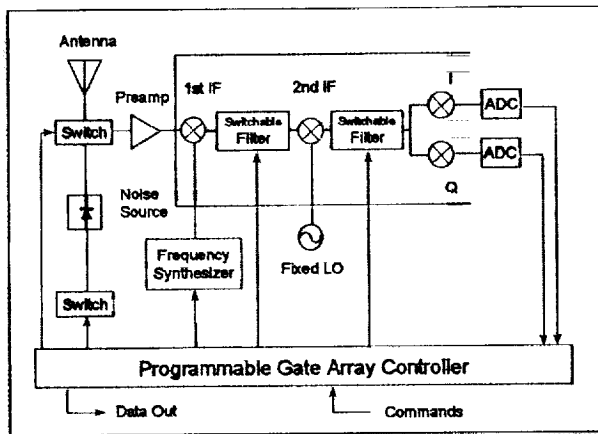


Figure 12. Block diagram of the final version of the EXPI/UMCP microreceiver.

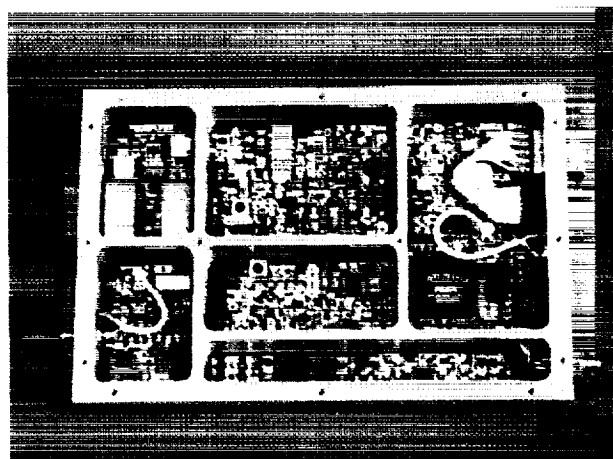


Figure 13. The final microreceiver prototype instrument with top cover removed.

Year 3 Meetings.

In October, 1998, Dr. Fry presented a paper on the microreceiver project (*A Mars Riometer*) at the American Astronomical Society/Division of Planetary Sciences annual meeting in Madison, WI. We held technical meetings in November at the University of Maryland, College Park, and at Data Design Corp. in Gaithersburg, MD. In December, Dr. Fry attended the American Geophysical Union meeting in San Francisco. He presented a paper (*A Programmable Riometer Receiver for Earth and Mars*) describing the microreceiver's riometer mode of operation. Dr. Fry met with Prof. Rosenberg and staff on April 5th, 1999, at the University of Maryland's College Park campus to discuss the McMurdo test data, and to review plans for the coming quarter. On June 3d, Dr. Fry presented a poster at the Spring AGU meeting in Boston (*Mars Prototype Riometer: First Operational Results From Antarctica*). Dr. Fry attended the 5th International Mars Conference at Cal Tech during the week of July 19th. On August 10th, Dr. Fry and Ms. Susan Fry (EXPI President) met in Lowell, MA, with Dr. Poole and Ms. Lee-Anne McKinnell of Rhodes University, and Dr. Kohichiro Oyama, of the Japanese ISAS, to discuss ionosonde requirements for a Mars lander and a Mars or Venus orbiter.

5.0 SUMMARY

We have successfully developed a programmable radio receiver that can be operated as a riometer and as a swept-frequency, VLF/HF radio spectrometer. The radio receiver, calibration, data acquisition and processing, and command and control functions are all contained on a single circuit board suitable for miniaturizing as a complete flight instrument.

In the first year, work focused on designing and building a breadboard receiver that implemented the riometer design. We were able to significantly miniaturize the receiver by using modern, low-power electronic components that have come on the market. We also implemented several of the subsystems in a field-programmable gate array (FPGA), including the receiver detector, the control logic, and the data acquisition and processing blocks.

In the second year, we evaluated the performance of the riometer mode in our lab and at the UMCP Beltsville field site, and modified the receiver design to incorporate the BBR mode. Considerable efforts were made to reduce the power consumption of the instrument, and eliminate or minimize RF noise and spurious emissions generated by the receiver's digital circuitry. We also made a number of design changes to decrease the receiver's power consumption.

In the third year, we deployed our prototype instrument at McMurdo Station, Antarctica, and operated it in parallel with a traditional riometer instrument for approximately two weeks. We ran a number of radio propagation simulations to finalize receiver specifications for the Mars version of the instrument. We determined that an instrument based upon an advanced chirp sounding technique would be most suitable for a Mars surface-based ionosonde. This technique allows an ionosonde to be built that is smaller in mass and consumes less power than competing instruments. The attached paper (accepted for publication by *Radio Science*) describes in detail the microreceiver theory of operation, performance specifications and test results.

Acknowledgements: This work was performed under NASA Planetary Instruments Definition and Development Contract NASW-96019. The authors appreciate beneficial discussions with E. Nielsen, P. Stauning, and A. W. V. Poole.

REFERENCES

- Barry, G. H., "A Low Power Vertical-Incidence Ionosonde," *IEEE Trans. Geosci. Electron.*, GE-9(2), pp. 86-89, 1971.
- Bougeret, J.-L., M. L. Kaiser, P. J. Kellogg, R. Manning, K. Goetz, S. J. Monson, N. Monge, L. Friel, C. A. Meetre, C. Perche, L. Sitruk and S. Hoang, "WAVES: The Radio and Plasma Wave Investigation on the Wind Spacecraft," *Space Sci. Rev.*, 71, pp. 231, 1995.
- Croft, T. A. and H. Hoogasian, "Exact Ray Calculations in a Quasi-Parabolic Ionosphere with no Magnetic Field," *Radio Science*, 3, 69-84, 1968.
- Cummer, S. and W. M. Farrell, "Radio Atmospheric Propagation on Mars and Potential Remote Sensing Applications," *J. Geophys. Res.*, 104, pp. 14,149-14,157, 1999.
- Detrick, D. L., and T. J. Rosenberg, "A Phased-Array Radiowave Imager for Studies of Cosmic Noise Absorption," *Radio Science*, 25, pp. 325-338, 1990.
- Detrick, D. L., T. J. Rosenberg, and C. D. Fry, "Analysis of the Martian Atmosphere for Riometry," *Planet. Space Sci.*, 45, 289-94, 1997.

- Farrell, W. M., M. L. Kaiser, M. D. Desch, J. G. Houser, S. A. Cummer, D. M. Witt, and G. A. Landis, "Detecting Electrical Activity from Martian Dust Storms," *J. Geophys. Res.*, 104, pp. 3795-3801, 1999.
- Fry, C. D. and R. J. Yowell, "Over-the-Horizon Communications on Mars via HF Radio Propagation," paper presented at the *Case for Mars V Conference*, organized by the Boulder Cent. for Sci and Policy, Boulder, Colorado, May 26-29, 1993.
- Fry, C. D. and R. J. Yowell, "HF Radio on Mars," *Commun. Q.*, 4(2), pp. 13-23, 1994.
- Fry, C. D., T. J. Rosenberg, L. Lutz, D. L. Detrick, A. T. Weatherwax, E. Knouse, H. Breden, and J. Giganti, "A Programmable Riometer For Earth and Mars," *Radio Science*, in press, 1999a.
- Fry, C. D., T. J. Rosenberg, A. T. Weatherwax and D. L. Detrick, "An HF Propagation Model for the Martian Ionosphere", in preparation, 1999b.
- Jones, R. M. and J. J. Stephenson, *A Versatile Three-Dimensional Ray Tracing Computer Program for Radio Waves in the Ionosphere*, Office of Telecommunications Report 75-76, Department of Commerce, Washington, DC, October 1975.
- Justus, C. G., B. F. James, and D. L. Johnson, "Mars Global Reference Atmospheric Model (Mars-GRAM 3.34): Programmer's Guide," *NASA Tech. Memo 108509*, May, 1996.
- Justus, C. G., D. L. Johnson, and B. F. James, "A Revised Thermosphere for the Mars Global Reference Atmospheric Model (Mars-GRAM Version 3.4)," *NASA Tech. Memo 108513*, July, 1996.
- Kaiser, M. L., "A Low-Frequency Radio Survey of the Planets with RAE 2," *J. Geophys. Res.*, 82, pp. 1256-1260, 1977.
- Klimov, S. I., V. V. Kopeikin, V. V. Krasnoselskikh, A. M. Natanzon, and A. E. Reznikov, "On the Use of a Mobile Surface Radar to Study the Atmosphere and Ionosphere of Mars," *Adv. Space Res.*, 10(3-4), pp. 35-38, 1990.
- La Belle, J. and A. T. Weatherwax, "Ground-based Observations of LF/MF/HF Radio Waves of Auroral Origin," in *Physics of Space Plasmas*, (T. Chang, ed.), Scientific Publishers, Cambridge, pp. 223- 236, 1992.
- Little, C. G. and H. Leinbach, "The Riometer - A Device for the Continuous Measurement of Ionospheric Absorption," *Proc. IRE*, 47, 315, 1959.
- McNamara, L., Jones-Stephenson Ray Tracing Source Code, <ftp://ftp.ngdc.noaa.gov>, 1992.
- Melnik O. and M. Parrot, "Propagation of Electromagnetic Waves through the Martian Ionosphere," *J. Geophys. Res.*, 104, 12,705-12,714, 1999.
- Meyer C., A. H. Treiman and T. Kostiuik, Planetary Surface Instrument Workshop, Part 6, Atmospheres from Within, *LPI Tech. Rep. 95-05*, Lunar and Planet. Inst., Houston, 1995.
- Nielsen, E., W. I. Axford, T. Hagfors, H. Kopka, N. A. Armand, V. A. Andrianov, D. J. Shtern and T. Breus, "The 'Long Wavelength Radar' on the Mars-94 Orbiter," *Adv. Space Res.*, 15(4), pp. 163-178, 1995.

- Ono, T., H. Oya, A. Morioka, A. Kumamoto, K. Kobayashi, T. Obara and T. Nakagawa, "Plasma Waves and Sounder (PWS) Experiment onboard the Planet-B Mars Orbiter," *Earth Planets Space*, 50, 213-221, 1998.
- Parrot, M., J. G. Trotignon, J. L. Rauch, L. J. C. Woolliscroft, S. P. Kingsley, J. C. Cerisier, E. Blanc, C. D. Fry and R. J. Yowell, "An Ionospheric Sounder for the Mars Landers," *Planet. Space Sci.*, pp. 1451-1455, 1996.
- Poole, A. W. V., "On the Use of Pseudorandom Codes for "Chirp" Radar," *IEEE Trans. Antennas Propag.*, AP-27(4), 480-485, 1979.
- Poole, A. W. V., "Advanced Sounding 1. The FMCW Alternative, *Radio Science*, 20, pp. 1609-1616, 1985a.
- Poole, A. W. V., and G. P. Evans, "Advanced Sounding 2. First Results From an Advanced Chirp Ionosonde," *Radio Sci.*, 20, 1617-23, 1985b.
- Reinisch, B. W., D. M. Haines and W. S. Kuklinski, "The New Portable Digisonde for Vertical and Oblique Sounding," in *AGARD, Remote Sensing of the Propagation Environment*, pp. 13-46, 1992.
- Rosenberg, T. J. and J. R. Dudeney, "The Local Time, Substorm, and Seasonal Dependence of Electron Precipitation at L = 4 Inferred from Riometer Measurements," *J. Geophys. Res.*, 91, pp. 12,032-12,040, 1986.
- Rosenberg, T. J., D. L. Detrick, D. Venkatesan, and G. van Bavel, "A Comparative Study of Imaging and Broad-Beam Riometer Measurements: The Effect of Spatial Structure on the Frequency Dependence of Auroral Absorption," *J. Geophys. Res.*, 96, 17,803, 1991.
- Rosenberg, T. J., Z. Wang, A. S. Rodger, J. R. Dudeney, and K. B. Baker, "Imaging Riometer and HF Radar Measurements of Drifting F Region Electron Density Structures in the Polar Cap," *J. Geophys. Res.*, 98, 7757, 1993.
- Weatherwax, A. T., J. La Belle and M. L. Trimpi, "A New Type of Auroral Radio Emission Observed at Medium Frequencies (~1350-3700 kHz) Using Ground-Based Receivers," *Geophys. Res. Lett.*, 21, pp. 2753-56, 1994.
- Yowell, R. J., *Investigation of Radio Wave Propagation in the Martian Ionosphere Utilizing HF Sounding Techniques*, M.S. Thesis, Air Force Inst. of Technol., Wright-Patterson AFB, Ohio, June, 1996.
- Zhang, M. H. G., J. G. Luhmann, A. J. Kliore and J. Kim, "A Post-Pioneer Reassessment of the Martian Dayside Ionosphere as Observed by Radio Occultation Methods," *J. Geophys. Res.*, 95, 14,829, 1990a.
- Zhang, M. H. G., J. G. Luhmann and A. J. Kliore, "An Observational Study of the Nightside Ionospheres of Mars and Venus with Radio Occultation Methods," *J. Geophys. Res.*, 95, 17,095, 1990b.

ATTACHMENT

Paper: A Programmable Riometer for Earth or Mars

A programmable riometer for Earth and Mars

C. D. Fry,¹ T. J. Rosenberg,² L. Lutz,² D. L. Detrick,² A. T. Weatherwax,²
E. Knouse,^{3,4} H. Breden,³ and J. Giganti⁵

Abstract. We have developed a miniature radio receiver designed to operate as a relative ionospheric opacity meter (riometer). This project was funded by NASA as an enabling technology for future planetary radio science missions. We sought to reduce the instrument's size, mass, and power so that it would be practical for a Mars lander or rover mission. A recent study by our group indicates that a riometer might work well on Mars and offers a potentially rich science return. The technology also has immediate terrestrial applications. For example, the University of Maryland operates a chain of imaging riometers at the Automatic Geophysical Observatories (AGOs) in Antarctica. Our riometer includes features that are desirable for extended autonomous operation such as those with AGOs: low power consumption, wide dynamic range and linearity, computer command and data interface, and the ability to be remotely reconfigured. The receiver design provides significant improvements over previous implementations used in riometers. The high degree of system linearity, combined with a digital feedback loop (including a low-duty calibration cycle), allows more time for viewing the radio sky. We implemented several of the receiver subsystems in a field-programmable gate array, including the receiver detector, the control logic, and the data acquisition and processing blocks. Considerable efforts were made to eliminate or minimize RF noise and spurious emissions generated by the receiver's digital circuitry. Results of laboratory and field tests are presented and discussed.

1. Introduction

There has been recent emphasis on reducing the size, cost, and development cycle of space systems, including instrumentation. Our group was funded by NASA to develop a versatile, multimode microreceiver. We sought to design a radio science instrument suitable for the class of missions falling in the NASA Mars Surveyor, Discovery, and New Millennium programs. Our goal was to miniaturize the electronics package so that

the instrument was practical for a Mars lander or rover mission. The first of three modes of operation to be incorporated into the microreceiver design allows the instrument to function as a riometer (relative ionospheric opacity meter). The riometer mode also forms the basis of a stand-alone instrument, and the Exploration Physics International/University of Maryland, College Park (EXPI/UMCP) programmable riometer is the first result of the microreceiver project.

1.1. Planetary Radio Science

Although much of terrestrial space science is conducted using orbiting satellites, ground-based ionospheric instruments continue to provide new information, not accessible from orbit, about the near-Earth space environment. None of these ground-based instru-

¹Exploration Physics International, Inc., Milford, New Hampshire.

²Institute for Physical Science and Technology, University of Maryland, College Park.

³Department of Physics, University of Maryland, College Park.

⁴Deceased March 10, 1999.

⁵Data Design Corporation, Gaithersburg, Maryland.

ments has ever been deployed on the surface of another planet, in spite of the potentially rich science return. Mars has a substantial daytime ionosphere, and some important features of the Martian ionosphere would be best observed from below. For example, by analogy with the terrestrial situation, solar energetic particle events, precipitating electrons, and meteors likely cause enhanced ionization in the lower Martian ionosphere. Ionospheric radars on orbiting spacecraft cannot measure the ionosphere below the height of the peak electron density, and radio occultation measurements are most sensitive to the ionosphere above about 90–100 km altitude. In addition, the Earth-Mars geometry precludes radio occultation measurements of the Martian ionosphere within about 45° of the subsolar point (and its antipode).

The riometer is a key instrument in ground-based studies of the terrestrial ionosphere. *Detrick et al.* [1997] compared the absorption of radio waves in the terrestrial and Martian atmospheres and concluded the riometer might also work well on Mars. The Planetary Surface Instruments Workshop [*Meyer et al.*, 1995] identified riometry as a practical technique for observing the Martian ionosphere and middle atmosphere. Listed below are several science goals our programmable riometer instrument might address and the relevant measurement objectives.

1.1.1. Space science. The goals in comparative aeronomy are to contribute to understanding Mars ionosphere-solar wind interactions, an outstanding problem in Mars aeronomy [*Luhmann*, 1995]; to apply riometry in an atmosphere different from that of the Earth; and to estimate ionospheric production and loss rates and energy deposition into the Martian middle atmosphere. The goals pertaining to energetic particles are to characterize and study precipitation of energetic particles and solar X rays; to determine the source of ionization of the nighttime Martian ionosphere, a key unknown at this time; and to measure absorption and thus the Martian atmosphere's response to ionizing events. The goals pertaining to microlightning are to detect and study in situ electrostatic discharge phenomena in Martian dust storms; to determine potential hazards to microelectronic components; and to measure the local RF noise environment for radio science and communications studies.

1.1.2. Human exploration and space development. The goals regarding radio wave propagation are to determine the potential for communications disruptions due to enhanced ionospheric absorption; and to measure RF absorption during solar X ray events

and from energetic particles (originating in the solar event/solar wind acceleration region). The goals pertaining to radiation hazard warnings are to evaluate the riometer as a solar proton warning system for Mars astronauts; and to measure enhancements in riometer absorption caused by the hard X ray flux and correlate them with absorption signatures of the solar energetic particles that often follow.

1.2. Terrestrial Radio Science

This technology also has applications for ground-based terrestrial ionospheric investigations. For example, the University of Maryland operates a chain of imaging riometers at the Automatic Geophysical Observatory (AGO) stations in Antarctica. Our receiver includes features that are desirable for extended autonomous operation such as those with AGOs: low power consumption, wide dynamic range and linearity, computer command and data interface, and the ability to be remotely reconfigured. Reductions in the power requirements and size of electronic components also allowed increased capabilities and versatility to be incorporated. The ability to perform for extended duration without operator intervention reduces maintenance requirements and the associated labor and travel costs.

In our design efforts, emphasis has been placed upon (1) minimizing the instrument size and mass by reducing the component count and other miniaturizing techniques, and (2) minimizing the operating power consumption by using a new breed of low-voltage devices. Our goal was to do all this without sacrificing instrument performance. By utilizing a field-programmable gate array, some receiver subsystems and digital signal processing functions are implemented in firmware. A serial interface allows commanding and programming of the receiver. The gate array also contains the onboard digital data acquisition system. An analog output is provided for testing and for compatibility with older data acquisition systems.

The following is a list of the key features of our programmable riometer (also see Table 1): reprogrammable receiver characteristics; tunable operating frequency over the range 0.1–25 MHz or 10–40 MHz, depending upon receiver configuration; self-calibration using a fixed-reference noise source at 30,000 K; improved immunity from intermodulation distortion; digital signal processor (DSP) detector stage, implemented in a field-programmable gate array (FPGA) integrated circuit; 12-bit analog-to-digital (A/D) conversion of receiver IF; 36-bit arithmetic computation and internal filtering algorithms; improved linearity over a wide dy-

locates the line along the high-level edge of the plot of superposed diurnal variations, which corresponds to the locus of inflection points for the voltage distributions at a series of times. When the riometer data are distributed in voltage, both high-signal-level (noise) and low-signal-level (large absorption) excursions lie far from the inflection point of the distribution and so do not affect the estimation of the quiet-day curve. Other automated techniques might not be so tolerant of such variations.

2.3. Riometry on Mars

Longwave (frequencies below 30 MHz) radio science instruments have flown on many interplanetary missions and have provided new understanding of interplanetary and planetary plasma processes [e.g., Kaiser, 1977; Warwick *et al.*, 1979; Barbosa, 1982; Stone *et al.*, 1992; Ladreiter *et al.*, 1994; Bougeret *et al.*, 1995]. In addition, the ill-fated Mars-94 spacecraft carried a longwave radar [Nielsen *et al.*, 1995], and a radio sounding instrument is on board the Planet-B/Nozomi mission [Ono *et al.*, 1998], now due to arrive at Mars in 2003–2004. Surface-based remote sensing of the Martian ionosphere, by means of HF radio, has only recently received attention [Klimov *et al.*, 1990; Meyer *et al.*, 1995; Parrot *et al.*, 1996; Detrick *et al.*, 1997]. As mentioned above, this is in part because of the previously prohibitive size of the radio instruments and required antennas.

Zhang *et al.* [1990a] reanalyzed radio occultation measurements of the Martian ionosphere from the Mariner 9 and Viking orbiter missions. Electron densities in the Martian ionosphere peak around $1\text{--}2 \times 10^5 \text{ cm}^{-3}$ during the day at an altitude of $\sim 135 \text{ km}$, yielding ionospheric critical frequencies of $\sim 3\text{--}4 \text{ MHz}$. The electron density profiles show considerable variations; the peak densities and heights of the peaks are remarkably similar from orbit to orbit. Maximum electron densities are much more irregular at night and drop to $\sim 10^3 \text{ cm}^{-3}$ or less [Zhang *et al.*, 1990b].

Surprisingly, there have been very few studies of LF–HF propagation in the Martian ionosphere. Fry and Yowell [1993, 1994] looked at oblique radio wave propagation using a quasi-parabolic ionospheric model, which provides exact solutions to the ray path equation [Croft and Hoogasian, 1968]. Yowell [1996] investigated the feasibility of using an ionospheric sounder on the surface of Mars to study radio wave propagation in the Martian ionosphere. Results of these studies indicate that during the daytime, radio wave propagation conditions on Mars are similar to those on Earth.

Detrick *et al.* [1997] evaluated the effects of enhanced ionization by precipitating electrons on radio frequency propagation through the Martian atmosphere. The dominant neutral molecule affecting radio wave absorption in the terrestrial atmosphere (to 200 km altitude) is N_2 , whereas CO_2 plays this role in the Martian atmosphere. The electron-neutral collision frequency (which determines the efficiency of absorbing radio waves) for CO_2 is at least an order of magnitude greater than for N_2 [Hake and Phelps, 1967] at temperatures present in the lower atmospheres of both planets. For this reason, it appears radio wave absorption is greater in the Martian atmosphere even though the neutral densities are less. The efficiency of an atmosphere to absorb radio waves (the term in the integral in equation (1), divided by n_e) is governed by the radio frequency and local effective collision frequency and is independent of the electron density. Figure 2, from data presented by Detrick *et al.* [1997], shows absorption efficiencies at a frequency of 40 MHz as a function of height in the terrestrial and Martian atmospheres.

3. Receiver Design

3.1. Conventional Riometer

A complete riometer instrument includes the self-calibrating radio receiver, a data acquisition system, and an external antenna. In traditional riometer design [Little and Leimbach, 1959; Chivers and Axford, 1973; Chivers, 1976] the receiver is continuously calibrated by rapidly switching the receiver input between a noise diode and the antenna. Differences between the diode and antenna noise levels produce a square wave signal at the switching frequency. This signal is detected in the receiver, integrated, and fed back to drive the noise diode so that its noise output matches the antenna's. The current through the diode is proportional to the noise power at the antenna. Absorption is then given by

$$A(\text{dB}) = -10 \log_{10} \frac{I}{I_0}, \quad (2)$$

where I is the measured noise diode current and I_0 is the quiet-day current expected at the same sidereal time (i.e., when absorption is minimized). With an integration time of 1 s and a bandwidth of about 250 kHz, receiver sensitivities are typically about 0.02 dB. The receiver is switched between the calibration diode and antenna at a 50% duty cycle. With modern receiver design, the current through the diode noise source can consume a significant fraction of the power provided to the instrument.

converter is only operated during the calibration cycle ($\sim 10\%$ of the time), at a time when the receiver output is dominated by the 30,000-K noise from the avalanche diode.

The receiver circuitry makes use of components designed for the cellular and portable RF link industries. Many of these components, while designed for low power consumption, do not perform well at high frequencies. We have found several which perform satisfactorily in the first and second mixers and in the frequency synthesizer.

All receiver, controller, and data acquisition electronics are contained in a single machined aluminum enclosure. The instrument enclosure is designed to minimize coupling between subsystems of the riometer. Presently, the dimensions of the enclosure are $10 \times 15 \times 2.5$ cm. For applications on Mars, we might significantly reduce the size of the flight instrument by utilizing a multilayer circuit board and multichip module design to meet volume (100 cm^3) and mass (100 g) design goals. The riometer draws less than 120 mW while operating.

3.4. Performance Considerations

Considerable effort went into decoupling the digital portions of the riometer from the RF front end. This is difficult to accomplish using a traditional DSP circuit. Conversely, we utilize the FPGA and drive it with a single synchronous clock, thus producing far less RF interference. The clock frequency is derived from the frequency synthesizer clock. This limits spurious generation of heterodyne frequencies produced by beating between oscillators. As a result, the injected noise lies below the noise floor of the receiver at our nominal operating frequency of 38.2 MHz. However, we expect there will be some degradation in performance at some frequencies, particularly those harmonically related to the gate array clock frequency. Other efforts to contain the injected noise include isolation of ground planes, extensive decoupling of signals between compartments containing the various receiver subsystems, and controlling the slew rate of the gate array input/output signals.

Several other design features incorporated into the riometer offer improvements over previous riometer systems. These include a higher intermediate frequency and sharper IF filters to significantly reduce the receiver's susceptibility to interfering signals.

4. Riometer Operation

The receiver measures the intensity of cosmic radio noise at the antenna input. It is calibrated by periodically switching between the antenna input and a known, stable noise source. Sky noise is determined by comparing the signal received at the antenna with the signal from the noise source. Ionospheric absorption is determined by comparing the present received power with the quiet-day curve. The FPGA measures a voltage proportional to the total RF power received at the antenna.

4.1. Theory of Operation

The receiver can be tuned on either side of a desired frequency to avoid interfering signals. Receiver parameters such as power bandwidth (nominally 50 kHz), calibration options, and operating mode can be programmed into the FPGA. Commands are input to the FPGA, and data are output using serial RS-232-C data words. In addition, other receiver characteristics are programmable, such as data sample rate and integration time constant and interval. For example, an integration time of 5 s allows the noise power to be measured with an accuracy of better than 0.01 dB. The minimum time constant is 0.1 s, allowing absorption measurements with an accuracy of 0.06 dB. Nominally, a 12-bit sample is output once every 5 s, although the sample rate may be varied. The instrument provides a serial RS-232-C data stream as well as an analog output. The output digital data samples are contained in three word frames, with a sync bit indicating the first word. The nominal data rate is 9600 bits per second. The data may be compressed through onboard processing and event thresholding.

There are several selectable operating modes: fixed-frequency, stepped frequency, and swept frequency. In the fixed-frequency mode, the bit pattern corresponding to one specific operating frequency is sent by the FPGA to the frequency synthesizer. A default frequency is selected when the riometer is switched on or when it is reset. In the stepped-frequency mode, a limited number of specific frequency channels are selected sequentially (for example, 20, 25, and 40 MHz). In the swept-frequency mode, the controller sends frequency commands to the synthesizer at a fixed rate, causing the receiver to be tuned over its entire range. To allow autonomous operation, the receiver can be commanded to search several adjacent frequencies around the desired one and to select the channel with the lowest noise.

Instantaneous power is computed from the vector

Fewer spikes appear in Figure 6, indicating that our new riometer was less susceptible to this particular RF interference than the conventional design instrument, probably as a result of the higher intermediate frequency (70 MHz versus 10.7 MHz) and the improved out-of-band rejection provided by the SAW filter in the IF stage. The narrower bandwidth (50 kHz versus 250 kHz) may also have contributed to some reduction of the interference.

6. Discussion and Conclusion

This report describes the design and operation of a radio receiver that forms the basis of a next-generation riometer. Our receiver design is significantly different from those used in previous riometer instruments. We use a field-programmable gate array to perform the detector, data acquisition, data processing, communications, and control functions. This significantly reduces the receiver's component count, which consequently reduces the instrument's size, mass, and power consumption.

We have met most of the design goals for the riometer mode of our microreceiver instrument. The receiver appears to perform well in both the laboratory tests and initial field tests. The power consumption is still about 20% higher than our original objective. Future development efforts will address the power issue and focus on extending the upper range of the receiver to 100 MHz. This will allow ionospheric absorption measurements to be made during the higher-energy proton events. These events can completely saturate the absorption signature at the lower operating frequencies. We will modify the frequency synthesizer circuit, move the first IF to a higher frequency, and expand the bandwidth of the front-end preamplifier. This will effectively require a redesign of the receiver. We also hope to increase the data processing capabilities on the gate array and to include some data compression and autonomous determination of the quiet-day curve. We will investigate further miniaturizing the receiver by implementing the RF and digital subsystems on a multichip module and other advanced electronics packaging techniques. Although this instrument was developed under NASA funding for future planetary radio science missions, the technology also has immediate terrestrial applications.

Since the Mars CO₂ atmosphere appears to be a more efficient absorber of RF energy than the Earth's, we anticipate that a riometer instrument might work well on Mars. To make ionospheric absorption measurements, the riometer must operate at a location beneath the

ionosphere, such as on a lander or rover vehicle, or perhaps in an aerobot (balloon or airplane). In the past, the size, complexity, and power requirements of radio science instruments have argued against including them on Mars surface missions. The Detrick *et al.* [1997] study and the instrument development effort we describe here indicate that riometry is now a viable technique for Mars aeronomy studies. A Mars riometer could be used to study the effects of solar energetic particle deposition and precipitating electrons on the Martian atmosphere and plasma environment. Comparisons with what we have learned about the terrestrial space environment would increase our understanding of both planets.

Acknowledgments. This work was performed as part of the development of a multifunction microreceiver for planetary radio science investigations, under NASA Planetary Instruments Definition and Development Contract NASW-96019. National Science Foundation grant OPP-9732662 also contributed to this project. The authors appreciate beneficial discussions with H. Chivers, E. Nielsen, and P. Stauning. We also acknowledge the helpful contributions of J. Etter, of the University of Maryland.

References

- Armstrong, T. P., C. M. Laird, D. Venkatesan, S. Krishnaswamy, and T. J. Rosenberg, Interplanetary energetic ions and polar radio wave absorption, *J. Geophys. Res.*, **94**, 3543, 1989.
- Barbosa, D. D., Low-level VLF and LF radio emissions observed at Earth and Jupiter, *Rev. Geophys.*, **20**, 316, 1982.
- Bougeret, J.-L., et al., WAVES: The radio and plasma wave investigation on the Wind spacecraft, *Space Sci. Rev.*, **71**, 231, 1995.
- Cane, H. V., A 30 MHz map of the whole sky, *Aust. J. Phys.*, **31**, 561, 1978.
- Chivers, H. J. A., and W. I. Axford, An investigation of high latitude ionospheric absorption, *Antarct. J. U.S.*, **7**, 244, 1973.
- Chivers, H. J. A., Substorm observations at $L = 4$, *Mem. Nat. Inst. Polar Res., Spec. Issue 6, Jpn.*, **76**, 1976.
- Croft, T. A., and H. Hoogasian, Exact ray calculations in a quasi-parabolic ionosphere with no magnetic field, *Radio Sci.*, **3**, 69, 1968.
- Davies, K., *Ionospheric Radio Waves*, Peter Peregrinus, London, 1990.
- Detrick, D. L., and T. J. Rosenberg, A phased array radio wave imager for studies of cosmic noise absorption, *Radio Sci.*, **25**, 325, 1990.
- Detrick, D. L., T. J. Rosenberg, and C. D. Fry, Analysis of the Martian atmosphere for riometry, *Planet. Space Sci.*, **45**, 289, 1997.
- Fry, C. D., and R. J. Yowell, Over-the-horizon communica-

Table 1. Programmable Riometer Specifications

Parameter	Specification
Frequency range	configurable (0.1–25 MHz or 10–40 MHz)
Detection mode	12-bit (analog-to-digital conversion for inphase and quadrature IF outputs) 36-bit (square law and filtering algorithm in gate array logic)
Detector dynamic range	45 dB (sinusoidal input) 35 dB (random noise input)
Noise figure	2 dB (at 40 MHz) and 5 dB (at 3 MHz)
Third-order intercept	-8 dBm
Bandwidth	50-kHz broadband, 15-kHz narrowband
Intermediate frequency	70 MHz
Tuning steps	Baseband inphase and quadrature channel (dc to 50 kHz) > 700 steps (nominal 60 kHz when upper frequency set at 40 MHz)
Detection time constant	10 ms to several seconds (selectable by command)
Gain stability	calibrated 30,000-K noise source is switched into receiver input with a 10% duty cycle; gain is controlled to obtain a constant output for this source
Zero calibration	50-ohm termination is switched into receiver input; receiver front-end noise is sampled and subtracted from the output power measurement
Outputs	analog output: 12-bit representation of received power (this signal provides the full dynamic range); digital output: RS232-C, 20-bit output from the gate array digital signal processor provided as three successive words
Controls	four-pole dip switch for default mode selection
Power	3 V at 120 mW
Enclosure	10 × 15 × 2.5 cm (4 × 6 × 1 inch) aluminum
Connectors	digital interface and data (nine-pin D style); receiver input (SMB coaxial); analog received power output (SMB coaxial); polarized four-pin power input connector

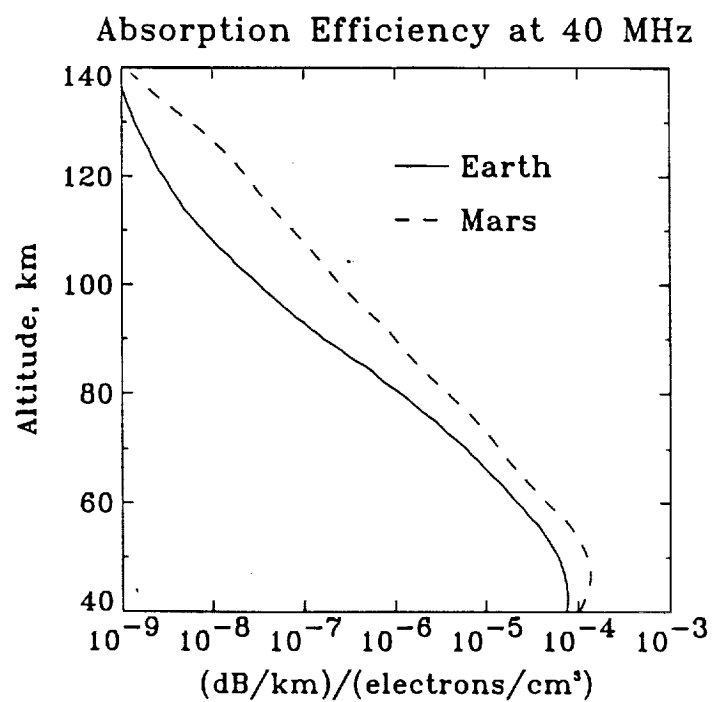


Figure 2. Comparison of radio wave absorption efficiencies at 40 MHz for the terrestrial and Martian atmospheres. Data are from *Detrick et al.* [1997].

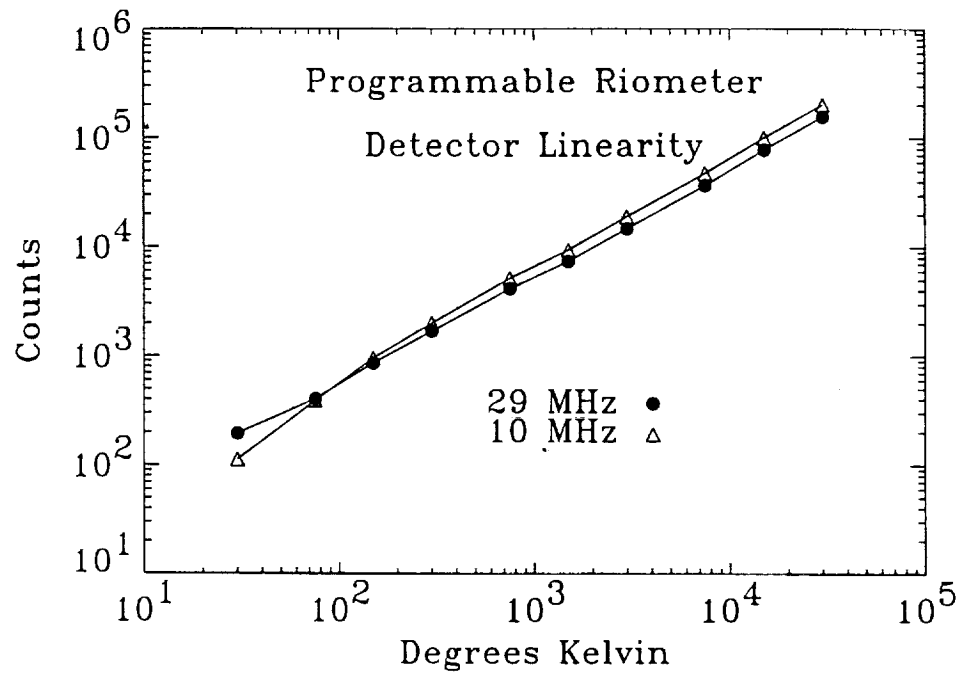


Figure 4. Laboratory measurements of detector linearity for random noise input at two frequencies.

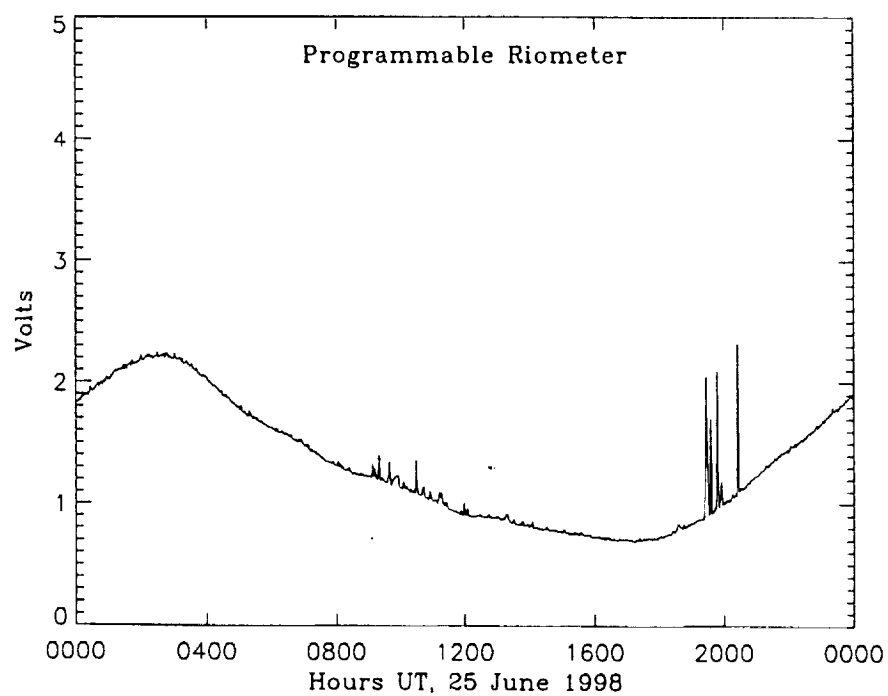


Figure 6. Programmable riometer output collected in parallel with the La Jolla Sciences, Inc. data for the same period as Figure 5. Note the lower levels of noise interference.

REPORT DOCUMENTATION PAGEForm Approved
OMB No. 0704-0188

Public reporting burden for this collection of information is estimated to average 1 hour per response, including the time for reviewing instructions, searching existing data sources, gathering and maintaining the data needed, and completing and reviewing the collection of information. Send comments regarding this burden estimate or any other aspect of this collection of information, including suggestions for reducing this burden, to Washington Headquarters Services, Directorate for Information Operations and Reports, 1215 Jefferson Davis Highway, Suite 1204, Arlington, VA 22202-4302, and to the Office of Management and Budget, Paperwork Reduction Project (0704-0188), Washington, DC 20503.

1. AGENCY USE ONLY (Leave blank)		2. REPORT DATE October 26, 1999	3. REPORT TYPE AND DATES COVERED Final Report, 10/8/96 - 10/7/99
4. TITLE AND SUBTITLE A Versatile Planetary Radio Science Micro-Receiver, Contract NASW-96019, Milestone Progress Report			5. FUNDING NUMBERS
6. AUTHORS C. D. Fry, T. J. Rosenberg*			
7. PERFORMING ORGANIZATION NAME(S) AND ADDRESS(ES) Exploration Physics International, Inc. (EXPI) 586-3 Nashua Street, Suite 222 Milford, NH 03055-4992			8. PERFORMING ORGANIZATION REPORT NUMBER C96-01AR03
9. SPONSORING/MONITORING AGENCY NAME(S) AND ADDRESS(ES) National Aeronautics and Space Administration Washington, DC 20546			10. SPONSORING/MONITORING AGENCY REPORT NUMBER
11. SUPPLEMENTARY NOTES Prepared by EXPI. *Institute for Physical Science and Technology, Univ. Maryland at College Park, MD			
12a. DISTRIBUTION/AVAILABILITY STATEMENT Unclassified - Unlimited			12b. DISTRIBUTION CODE
13. ABSTRACT (Maximum 200 words) We have developed a low-power, programmable radio "microreceiver" that combines the functionality of two science instruments: a Relative Ionospheric Opacity Meter (riometer) and a swept-frequency, VLF/HF radio spectrometer. The radio receiver, calibration noise source, data acquisition and processing, and command and control functions are all contained on a single circuit board. This design is suitable for miniaturizing as a complete flight instrument. Several of the subsystems were implemented in a field-programmable gate array (FPGA), including the receiver detector, the control logic, and the data acquisition and processing blocks. Considerable efforts were made to reduce the power consumption of the instrument, and eliminate or minimize RF noise and spurious emissions generated by the receiver's digital circuitry. A prototype instrument was deployed at McMurdo Station, Antarctica, and operated in parallel with a traditional riometer instrument for approximately three weeks. The attached paper (accepted for publication by <i>Radio Science</i>) describes in detail the microreceiver theory of operation, performance specifications and test results.			
14. SUBJECT TERMS Riometer, Broadband Receiver, Remote Sensing, Mars Atmosphere, Planetary Instruments, Martian ionosphere, ionosonde			15. NUMBER OF PAGES
			16. PRICE CODE
17. SECURITY CLASSIFICATION OF REPORT Unclassified	18. SECURITY CLASSIFICATION OF THIS PAGE Unclassified	19. SECURITY CLASSIFICATION OF ABSTRACT Unclassified	20. LIMITATION OF ABSTRACT Unlimited